Dileptons from the nonequilibrium Quark-Gluon Plasma

E. L. Bratkovskaya[a], O. Linnyk[a] and W. Cassing[b]

[a]Institut für Theoretische Physik, Universität Frankfurt, 60438 Frankfurt am Main, Germany
[b]Institut für Theoretische Physik, Universität Giessen, 35392 Giessen, Germany

Abstract. According to the dynamical quasiparticle model (DQPM) – matched to reproduce lattice QCD results in thermodynamic limit, – the constituents of the strongly interacting quark-gluon plasma (sQGP) are massive and off-shell quasi-particles (quarks and gluons) with broad spectral functions. In order to address the electromagnetic radiation of the sQGP, we derive off-shell cross sections of $q\bar{q} \to \gamma^*$, $q\bar{q} \to \gamma^* + g$ and $qg \to \gamma^* q (\bar{q}g \to \gamma^* \bar{q})$ reactions taking into account the effective propagators for quarks and gluons from the DQPM. Dilepton production in In+In collisions at 158 AGeV is studied by implementing these processes into the parton-hadron-string dynamics (PHSD) transport approach. The microscopic PHSD transport approach describes the full evolution of the heavy-ion collision: from the dynamics of quasi-particles in the sQGP phase (when the local energy density is above ~ 1 GeV/fm^3) through hadronization and to the following hadron interactions and off-shell propagation after the hadronization. A comparison to the data of the NA60 Collaboration shows that the low mass dilepton spectra are well described by including a collisional broadening of vector mesons, while the spectra in the intermediate mass range are dominated by off-shell quark-antiquark annihilation, quark Bremsstrahlung and gluon-Compton scattering in the nonperturbative QGP. In particular, the observed softening of the m_T spectra at intermediate masses (1 GeV $\leq M \leq$ 3 GeV) is approximately reproduced.

1. Introduction

While the properties of hadrons are rather well known in free space (embedded in a nonperturbative QCD vacuum) the masses and lifetimes of hadrons in a baryonic and/or mesonic environment are subject of current research in order to achieve a better understanding of the strong interaction and the nature of confinement. A modification of vector mesons has been seen experimentally in the enhanced production of lepton pairs above known sources in nucleus-nucleus collisions at Super-Proton-Synchroton (SPS) energies [1, 2]. This can be attributed to a shortening of the lifetime of the vector mesons ρ, ω and ϕ. The question arises if the enhancement might (in part) be due to new radiative channels [3] from the strong Quark-Gluon Plasma (sQGP). The answer to this question is nontrivial due to the nonequilibrium nature of the heavy-ion reactions and covariant transport models have to be incorporated to disentangle the various sources that contribute to the final dilepton spectra seen experimentally.

2. The PHSD approach

To address the vector meson properties in a hot and dense medium – as created in heavy-ion collisions – we employ an up-to-date relativistic transport model, i.e. the Parton Hadron String Dynamics model [4] (PHSD) that incorporates the relevant off-shell dynamics of the vector

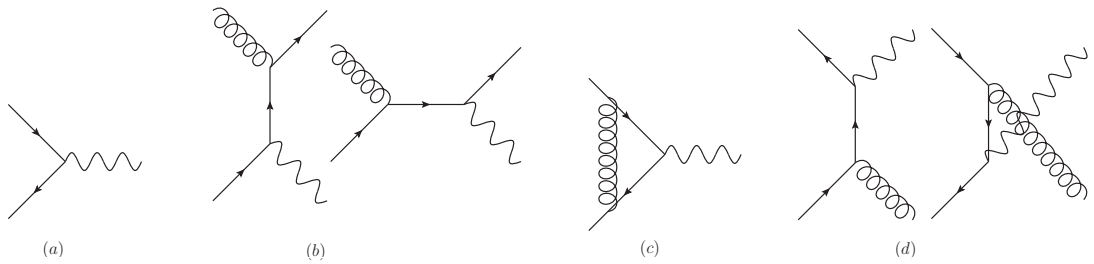

Figure 1. Diagrams contributing to the dilepton production from a QGP: (a) Drell-Yan mechanism, (b) gluon-Compton scattering (GCS), (c) vertex correction, (d) gluon Bremsstrahlung (NLODY), where virtual photons (wavy lines) split into lepton pairs, spiral lines denote gluons, arrows denote quarks. In each diagram the time runs from left to right.

mesons as well as the explicit partonic phase in the early hot and dense reaction region. PHSD consistently describes the full evolution of a relativistic heavy-ion collision from the initial hard scatterings and string formation through the dynamical deconfinement phase transition to the quark-gluon plasma (QGP) as well as hadronization and to the subsequent interactions in the hadronic phase.

In the hadronic sector PHSD is equivalent to the Hadron-String-Dynamics (HSD) transport approach [5, 6, 7] that has been used for the description of pA and AA collisions from SIS to RHIC energies and has lead to a fair reproduction of hadron abundances, rapidity distributions and transverse momentum spectra. In particular, HSD incorporates off-shell dynamics for vector mesons – according to Refs. [8] – and a set of vector-meson spectral functions [10] that covers possible scenarios for their in-medium modification. The transport theoretical description of quarks and gluons in PHSD is based on a dynamical quasiparticle model for partons matched to reproduce lattice QCD results in thermodynamic equilibrium (DQPM). The transition from partonic to hadronic degrees of freedom is described by covariant transition rates for the fusion of quark-antiquark pairs to mesonic resonances or three quarks (antiquarks) to baryonic states.

Various models predict that hadrons change in the (hot and dense) nuclear medium; in particular, a broadening of the spectral function or a mass shift of the vector mesons has been expected. Furthermore, QCD sum rules indicated that a mass shift may lead to a broadening and vice versa [9]; therefore both modifications should be studied simultaneously. Thus we explore three possible scenarios: (1) a broadening of the ρ spectral function, (2) a mass shift, and (3) a broadening plus a mass shift. The HSD (PHSD) off-shell transport approach allows to investigate in a consistent way the different scenarios for the modification of vector mesons in a hot and dense medium. In off-shell transport the hadron spectral functions change dynamically during the propagation through the medium and evolve towards the on-shell spectral function in the vacuum.

As demonstrated in Ref. [10] the off-shell dynamics is particularly important for resonances with a rather long lifetime in vacuum but strongly decreasing lifetime in the nuclear medium (especially ω and ϕ mesons) but also proves vital for the correct description of dilepton decays of ρ mesons with masses close to the two pion decay threshold. For a detailed description of the various hadronic channels included for dilepton production as well as the off-shell dynamics we refer the reader to Refs. [10, 11].

3. SPS energies

By employing the HSD approach to the low mass dilepton production in relativistic heavy-ion collisions, it was shown in [11] that the NA60 Collaboration data for the invariant mass spectra for $\mu^+\mu^-$ pairs from In+In collisions at 158 A·GeV favored the 'melting ρ' scenario [13]. Also

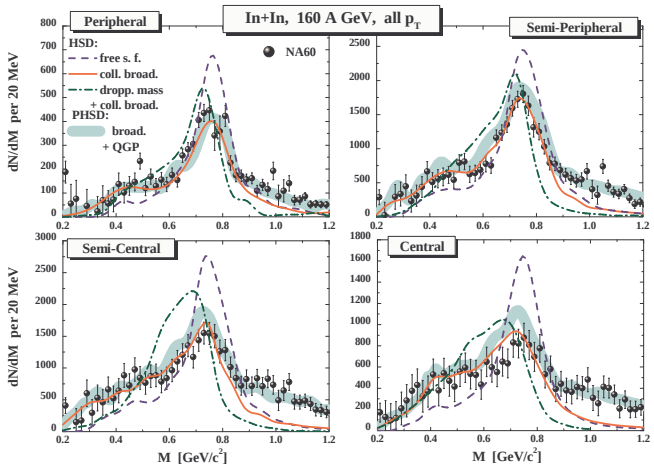

Figure 2. The HSD results for the mass differential dilepton spectra from $In + In$ collisions at 158 A·GeV in comparison to the excess mass spectrum from NA60 [13]. The actual NA60 acceptance filter and mass resolution have been incorporated [23]. The solid lines show the HSD results for a scenario including the collisional bradening of the ρ-meson whereas the dashed lines correspond to calculations with a 'free' ρ spectral functions for reference. The dash-dotted lines represent the HSD calculations for the 'dropping mass + collisional broadening' model. The bands represent the preliminary PHSD results incorporating direct dilepton radiation from the QGP in addition to a broadened ρ-meson.

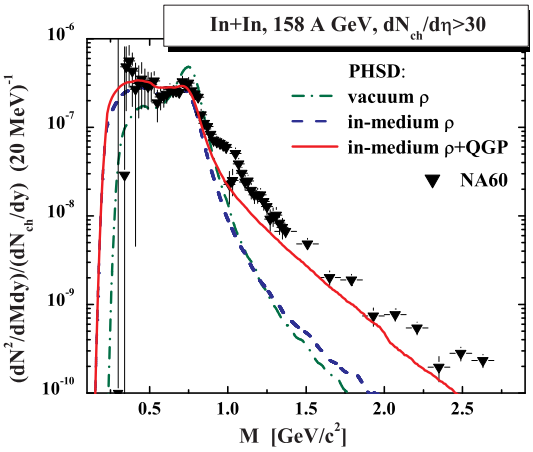

Figure 3. Acceptance corrected mass spectra of the excess dimuons from $In + In$ at 158 AGeV integrated over p_T in $0.2 < p_T < 2.4$ GeV from PHSD compared to the data of NA60 [15]. The green dash-dotted line shows the dilepton yield from the vacuum ρ meson. The blue dashed line is the contribution to the dilepton yield from the in-medium ρ with broadened spectral function. The red solid line presents the sum of the in-medium ρ and QGP dilepton radiation (the latter is calculated in the on-shell approximation in this work).

the data from the CERES Collaboration [14] showed a preference for the 'melting ρ' picture. On the other hand, the dilepton spectrum from In+In collisions at 158 A·GeV for $M > 1$ GeV could not be accounted for by the known hadronic sources (see Fig.2 of [11]). Also, hadronic models do not reproduce the softening of the m_T distribution of dileptons for $M > 1$ GeV [13]. This observation pointed towards a partonic origin.

Dilepton radiation by the constituents of the strongly interacting QGP proceeds via the elementary processes illustrated in Fig. 1: the basic Drell-Yan $q + \bar{q}$ annihilation mechanism, Gluon Compton scattering ($q + g \to \gamma^* + q$ and $\bar{q} + g \to \gamma^* + \bar{q}$), and quark + anti-quark annihilation with gluon Bremsstrahlung in the final state ($q + \bar{q} \to g + \gamma^*$). In the on-shell approximation, one uses perturbative QCD cross sections for the processes listed above. The obtained off-shell elementary cross sections have been implemented into the PHSD transport code. Note that in our calculations the running coupling α_S depends on the local energy density ϵ according to the DPQM [12], while the energy density is related to the temperature T by the lQCD equation of state. Numerically, we observe that α_S is of the order $O(1)$ and thus the contribution of the higher order diagrams in Fig. 1 is not subleading!

As we find in Fig. 3 the NA60 data favor the scenario of the in-medium broadening of vector mesons. Note that in the data - presented in this plot - the D-meson contribution has not been subtracted. The NA60 collaboration has published acceptance corrected data with subtracted

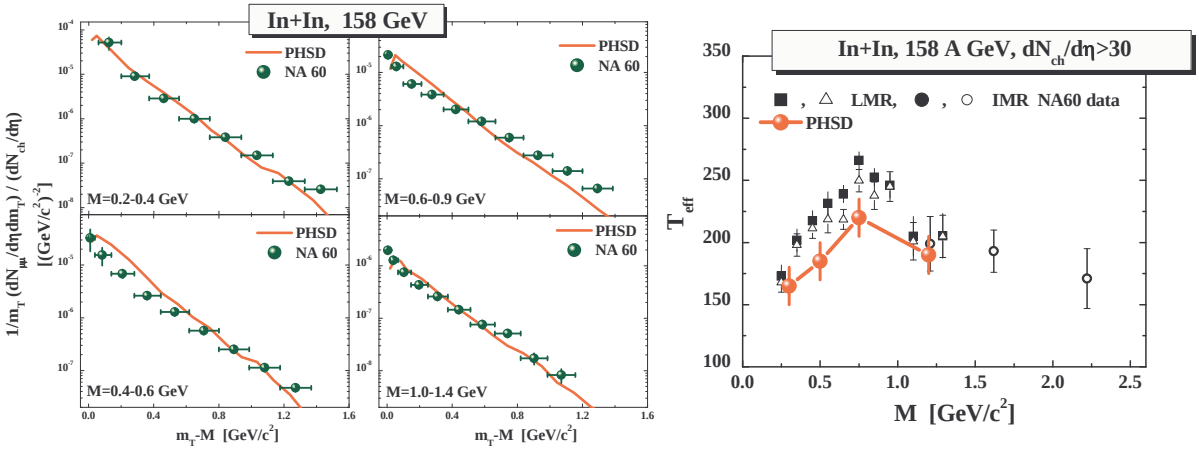

Figure 4. Left: Transverse mass spectra of dileptons for In+In at 158 A·GeV. **Right: Right:** The inverse slope parameter T_{eff} of the dimuon yield from In+In at 158 A·GeV as a function of the dimuon invariant mass in PHSD compared to the data of the NA60 Collaboration [13, 15].

charm contribution recently [15]. In Fig. 3 we present PHSD results for the dilepton spectrum excess over the known hadronic sources as produced in $In+In$ reactions at 158 AGeV compared to the acceptance corrected data. We find that the spectrum at invariant masses below 1 GeV is well reproduced by the ρ meson yield, if a broadening of the meson spectral function in the medium is assumed. On the other hand, the spectrum at $M > 1$ GeV is shown to be dominated by the partonic sources.

It is also interesting to note that accounting for partonic dilepton sources allows to reproduce in PHSD (cf. Fig. 3, rhs) the intriguing finding of the NA60 Collaboration [13, 15] that the effective temperature of the dileptons (slope parameters) in the intermediate mass range is lower than the T_{eff} of the dileptons from the hadronic phase. The softening of the transverse mass spectrum with growing invariant mass reflects that the partonic channels occur dominantly before the collective radial flow has developed. This feature of the data is also reproduced in PHSD (cf. Fig. 4, rhs). A detailed look at the PHSD results shows that in total we still underestimate the slope parameter T_{eff} which might be due to missing partonic initial state effects or an underestimation of partonic flow in the initial phase of the reaction.

4. RHIC energies

In 2008, the PHENIX Collaboration has presented first dilepton data from pp and $Au + Au$ collisions at Relativistic-Heavy-Ion-Collider (RHIC) energies of $\sqrt{s} = 200$ GeV [17] which show an even larger enhancement in $Au+Au$ reactions (relative to pp collisions) in the invariant mass regime from 0.15 to 0.6 GeV than the data at SPS energies [13, 14]. We recall that HSD provides a reasonable description of hadron production in $Au+Au$ collisions at $\sqrt{s} = 200$ GeV [19] such that we can directly continue with the results for e^+e^- pairs which are shown in Fig. 5 for $p+p$ collisions. We find that the dilepton radiation in the elementary channel is well under control in HSD, which is equivalent to PHSD for $p+p$ reactions.

We step on with the case of inclusive $Au + Au$ collisions in comparison to the data from PHENIX [17] (Fig 6). When including the in-medium modification scenarios for the vector mesons, we achieve a sum spectrum which is only slightly enhanced compared to the 'free' scenario. Whereas the total yield is quite well described in the region of the pion Dalitz decay as well as around the ω and ϕ mass, HSD clearly underestimates the measured spectra in the regime from 0.2 to 0.6 GeV by an average factor of ~ 3. The low mass dilepton spectra from

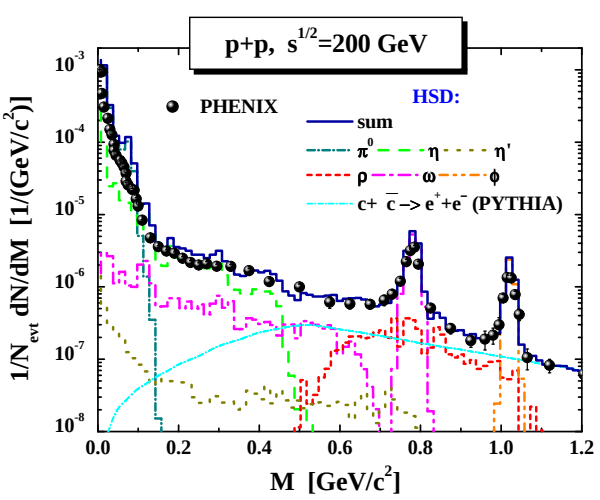

Figure 5. The HSD results for the mass differential dilepton spectra in case of pp collisions at $\sqrt{s}$ = 200 GeV in comparison to the data from PHENIX [16]. The actual PHENIX acceptance and mass resolution have been incorporated (see legend for the different color coding of the individual channels). Figure taken from [11].

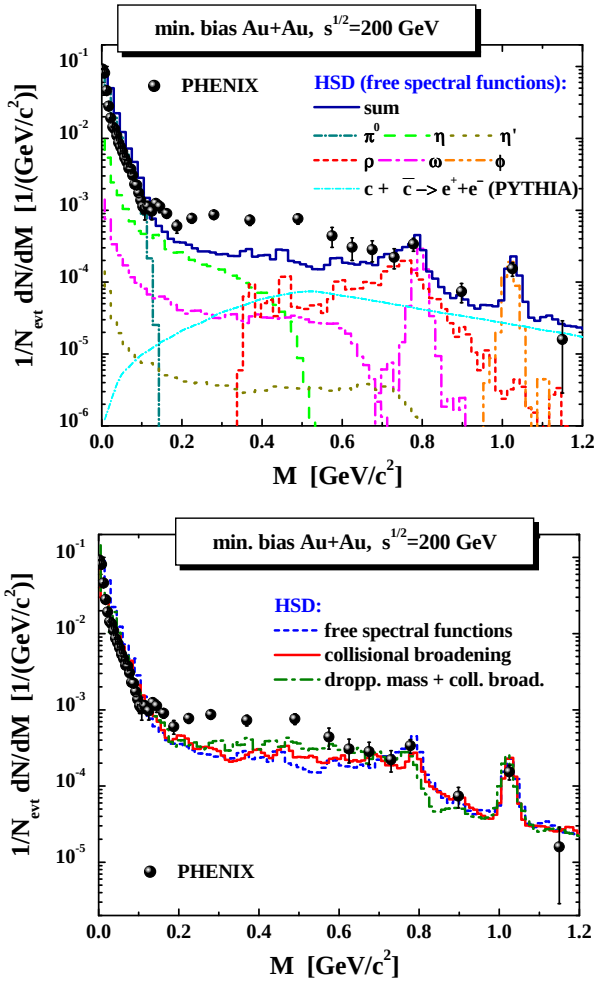

Figure 6. The HSD results for the mass differential dilepton spectra in case of inclusive $Au + Au$ collisions at $\sqrt{s}$ = 200 GeV in comparison to the data from PHENIX [17]. The actual PHENIX acceptance filter and mass resolution have been incorporated [18]. In the upper part the results are shown for vacuum spectral functions (for ρ, ω, ϕ) including the channel decompositions (see legend for the different color coding of the individual channels). The lower part shows a comparison for the total e^+e^- mass spectrum in case of the 'free' scenario (dashed line), the 'collisional broadening' picture (solid line) as well as the 'dropping mass + collisional broadening' model (dash-dotted line). Figure taken from [11].

$Au+Au$ collisions at RHIC (from the PHENIX Collaboration) are clearly underestimated in the invariant mass range from 0.2 to 0.6 GeV in the 'collisional broadening' scenario as well as in the 'dropping mass + collisional broadening' model, i.e. when assuming a shift of the vector meson mass poles with the baryon density. We mention that our results for the low mass dileptons are very close to the calculated spectra from van Hees and Rapp [20] as well as Dusling and Zahed [21] (cf. the comparison in Ref. [22]).

Consequently we attribute this additional low mass enhancement seen by PHENIX to non-hadronic sources. This assumption has to be tested quantitatively. However, in order to make quantitative predictions at experimentally relevant low dilepton mass ($\leq$ 0.6 GeV) and strong coupling ($\alpha_S \sim 0.5 \div 1$), we have to take into account not only the higher order pQCD reaction mechanisms, but also the non-perturbative spectral functions and self-energies of the quarks,

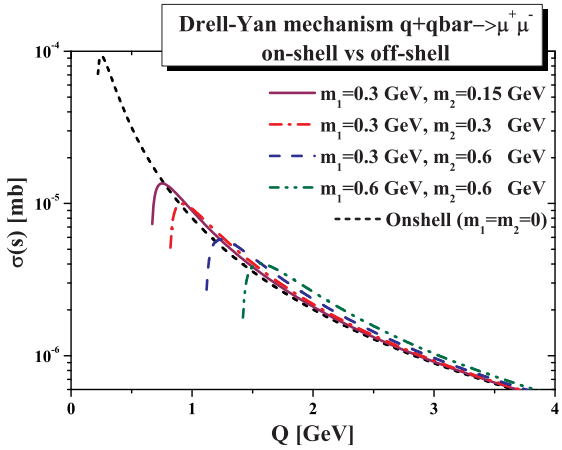

Figure 7. Dilepton production cross sections in the Drell-Yan channel ($q + \bar{q} \to \mu^+ + \mu^-$). The short dashes (black) line shows the on-shell, i.e. the standard pQCD result. The other lines show the off-shell cross section, in which the annihilating quark and antiquark have finite masses m_1 and m_2 with different values: $m_1 = 0.3$ GeV, $m_2 = 0.15$ GeV (solid magenta line), $m_1 = 0.3$ GeV, $m_2 = 0.3$ GeV (dash-dotted red line), $m_1 = 0.3$ GeV, $m_2 = 0.6$ GeV (dashed blue line), $m_1 = 0.6$ GeV, $m_2 = 0.6$ GeV (dash-dot-dot green line).

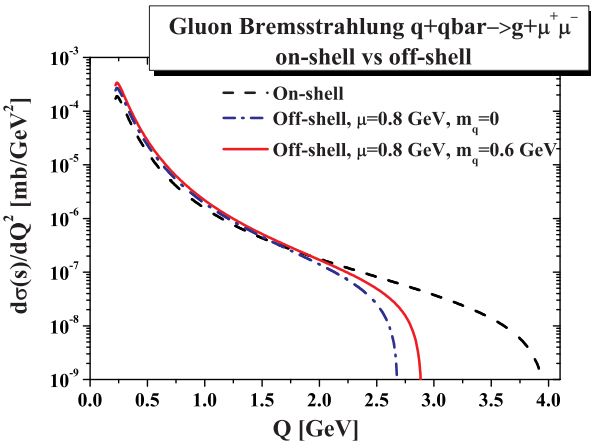

Figure 8. Comparison of off-shell and on-shell cross sections for dilepton production in the gluon Bremsstrahlung $q + \bar{q} \to g + \mu^+\mu^-$ channel at $\sqrt{s} = 4$ GeV. The dashed black line shows the on-shell (pQCD) cross section regularized by the cut on the gluon mass $\mu_{cut} = 0.206$ GeV, the blue dash-dotted line presents the off-shell cross section for the gluon mass fixed to $\mu = 0.8$ GeV and on-shell quark and anti-quark ($m_1 = m_2 = m_3 = 0$). The red solid line gives the off-shell result for $\mu = 0.8$ GeV, $m_1 = m_2 = m_3 = m_q = 0.6$ GeV.

anti-quarks and gluons thus going beyond the leading twist.

For this purpose, off-shell cross sections were derived in [24] for dilepton production in the reactions $q + \bar{q} \to l^+l^-$ (Drell-Yan mechanism), $q + \bar{q} \to g + l^+l^-$ (quark annihilation with the gluon Bremsstrahlung in the final state), $q(\bar{q}) + g \to q(\bar{q}) + l^+l^-$ (gluon Compton scattering), $g \to q+\bar{q}+l^+l^-$ and $q(\bar{q}) \to q(\bar{q})+g+l^+l^-$ (virtual gluon decay, virtual quark decay) in the sQGP in effective perturbation theory by dressing the quark and gluon lines in the diagrams in Fig. 1 with the DQPM propagators for quarks and gluons. The DQPM describes QCD properties in terms of single-particle Green's functions (in the sense of a two-particle irreducible approach) and leads to the notion of the constituents of the sQGP being effective quasiparticles, which are massive and have broad spectral functions (due to large interaction rates).

Dilepton production cross sections in the Drell-Yan mechanism are plotted on the l.h.s. of Fig. 7. The short dashes (black) line shows the on-shell, i.e. the standard perturbative result. The other lines show the off-shell cross section, in which the annihilating quark and antiquark have finite masses m_1 and m_2 with different values: $m_1 = 0.3$ GeV, $m_2 = 0.15$ GeV (solid magenta line), $m_1 = 0.3$ GeV, $m_2 = 0.3$ GeV (dash-dotted red line), $m_1 = 0.3$ GeV, $m_2 = 0.6$ GeV (dashed blue line), $m_1 = 0.6$ GeV, $m_2 = 0.6$ GeV (dash-dot-dot green line).

In Fig. 8, the off-shell cross sections for the quark annihilation with gluon bremsstrahlung channel at various values of quark and gluon off-shellnesses (masses) are compared to the on-shell (pQCD) result. The dashed black line shows the on-shell cross section regularized by a cut on gluon mass $\mu_{cut} = 0.206$ GeV, the red solid line presents the off-shell cross section for the gluon mass fixed to $\mu = 0.8$ GeV and on-shell quark and anti-quark ($m_1 = m_2 = m_3 = 0$). The blue dash-dotted line gives the off-shell result for $\mu = 0.8$ GeV, $m_1 = m_2 = m_3 = m_q = 0.6$ GeV.

One readily notices the shift of the maximum allowed mass of the lepton pair to a lower value (in order to produce a massive gluon in the final state).

By implementing the off-shell partonic processes into the PHSD transport approach, a consistent calculation of the dilepton production in heavy-ion collisions at RHIC energies will be performed in near future. The comparison to the dilepton data double differentially in mass and p_T will open the possibility to study the relative importance of different processes in the dilepton production and guide us towards a better understanding of the properties of matter at high densities and temperatures as created in heavy-ion collisions.

5. Summary

Dilepton production in relativistic heavy-ion collisions is a valuable probe of two phenomena of fundamental interest: the vector meson properties in a hot and dense medium and of the quark and gluon dynamics in the deonfined state of matter (sQGP). The Parton Hadron String Dynamics [4] (PHSD) transport approach incorporates the relevant off-shell dynamics of the vector mesons as well as the explicit partonic phase in the early hot and dense reaction region.

A comparison of the transport calculations to the data of the CERES and NA60 Collaborations points towards 'melting' modification of the ρ'-meson at high densities, i.e. the broadening of the vector meson's spectral function. On the other hand, the spectrum for $M > 1$ GeV is shown to be dominated by the partonic sources.

The low mass dilepton spectra from $Au + Au$ collisions at RHIC (from the PHENIX Collaboration) are clearly underestimated by the hadronic channels in the invariant mass range from 0.2 to 0.6 GeV in the 'collisional broadening' scenario as well as in the 'dropping mass + collisional broadening' model, i.e. when assuming a shift of the vector meson mass poles with the baryon density. We attribute this additional low mass enhancement seen by PHENIX to radiation from the strongly interacting QGP. This assumption has to be tested quantitatively. Strong interaction of partons - reflected in their high masses and broad widths - lead to higher-twist corrections to the perturbative cross sections especially at the experimentally relevant low dilepton masses (≤ 0.6 GeV). By implementing the off-shell partonic processes into the PHSD transport approach, a consistent calculation of the dilepton production in heavy-ion collisions at RHIC energies will be performed in near future that will allow us answer whether the observed access can be attributed to the radiation by off-shell partons.

Acknowledgments

OL acknowledges financial support within the "HIC for FAIR" center of the "LOEWE" program.

References

[1] G. Agakichiev *et al.*, CERES Collaboration, *Phys. Rev. Lett.* **75** (1995) 1272; Th. Ullrich *et al.*, *Nucl. Phys.* A**610** (1996) 317c; A. Drees, *Nucl. Phys.* A**610** (1996) 536c.
[2] M. A. Mazzoni, HELIOS Collaboration, *Nucl. Phys.* A**566** (1994) 95c; M. Masera, *Nucl. Phys.* A**590** (1995) 93c; T. Åkesson et al., *Z. Phys.* C**68** (1995) 47.
[3] O. Linnyk, E. L. Bratkovskaya and W. Cassing, *Nucl. Phys.* A **830** (2009) 491C.
[4] W. Cassing and E. L. Bratkovskaya, *Phys. Rev.* C **78** (2008) 034919; *Nucl. Phys.* A **831** (2009) 215.
[5] W. Cassing, E. L. Bratkovskaya, *Phys. Rept.* **308** (1999) 65.
[6] E. L. Bratkovskaya, W. Cassing, *Nucl. Phys.* A**619** (1997) 413.
[7] W. Ehehalt, W. Cassing, *Nucl. Phys.* A **602** (1996) 449.
[8] W. Cassing, S. Juchem, *Nucl. Phys.* A **665** (2000) 377; *ibid.* A **672** (2000) 417.
[9] J. Ruppert, T. Renk and B. Müller, *Phys. Rev.* C 73 (2006) 034907.
[10] E. L. Bratkovskaya, W. Cassing, *Nucl. Phys.* A **807** (2008) 214.
[11] E. L. Bratkovskaya, W. Cassing and O. Linnyk, *Phys. Lett.* B **670** (2009) 428.
[12] W. Cassing, *Nucl. Phys.* A 791 (2007) 365; *ibid.* A 795 (2007) 70.
[13] R. Arnaldi *et al.*, NA60 Collaboration, *Phys. Rev. Lett.* **96** (2006) 162302; J. Seixas *et al.*, *J. Phys.* G **34** (2007) S1023; S. Damjanovic *et al.*, *Nucl. Phys.* **A 783** (2007) 327c.

[14] D. Adamova *et al.* CERES Collaboration, *Nucl. Phys.* A **715** (2003) 262; *Phys. Rev. Lett.* **91** (2003) 042301; G. Agakichiev *et al.*, *Eur. Phys. J.* C **41** (2005) 475; D. Adamova *et al. Phys. Lett.* B **666** (2008) 425; A. Marin *et al.*; Proceedings of CPOD07, PoS 034 (2007).
[15] R. Arnaldi *et al.*, NA60 Collaboration, Eur. Phys. J. C **59**, 607 (2009)
[16] A. Adare *et al.*, PHENIX Collaboration, *Phys. Lett.* B **670** (2009) 313
[17] A. Toia *et al.*, PHENIX Collaboration, *Nucl. Phys.* A **774** (2006) 743; *Eur. Phys.* J **49** (2007) 243; S. Afanasiev *et al.*, PHENIX Collaboration, arXiv:0706.3034 [nucl-ex]; A. Adare *et al.*, PHENIX Collaboration, arXiv:0912.0244 [nucl-ex].
[18] A. Toia, private communication.
[19] E. L. Bratkovskaya, W. Cassing, H. Stöcker, *Phys. Rev.* **C 67** (2003) 054905; E. L. Bratkovskaya *et al. Phys. Rev.* **C 69** (2004) 054907.
[20] H. van Hees, R. Rapp, Phys. Rev. Lett. **97** (2006) 102301.
[21] K. Dusling and I. Zahed, *Nucl. Phys.* A **825** (2009) 212.
[22] A. Toia, *J. Phys.* G **35** (2008) 104037.
[23] S. Damjanovic, private communication.
[24] O. Linnyk, arXiv:1004.2591 [hep-ph].